Kochi Chapter

Indian Geotechnical Conference
IGC 2022
15th – 17th December, 2022, Kochi

Experimental Investigation of the Micromechanical Interface Friction of Non-Dilative Geotechnical Interfaces

Lalit Kandpal[1], Prashanth Vangla[1], Satoshi Matsumura[2], and Nitya Nand Gosvami[3]

[1]Department of Civil Engineering, Indian Institute of Technology Delhi, New Delhi, India
[2]Port and Airport Research Institute, Yokosuka, Japan
[3]Department of Materials Science and Engineering, Indian Institute of Technology Delhi, New Delhi, India
[1]lalitkandpal1996@gmail.com

Abstract. Load transfer from the structure to the surrounding soil is mainly through the frictional force at the contacts of the geotechnical composites incorporating non-dilative interfaces. The frictional mechanism is governed mainly by sliding and plowing actions and often do not follow the Amonton's law. Thus, understanding of the micromechanical behavior is essential in the modeling and actual field behavior of non-dilative interface systems. A series of experiments were conducted to study the frictional behavior of single particle and smooth continuum materials using a particle-on-disc tribometer. The tests were conducted at different normal loads (5 N, 10 N, 20 N, 40 N and 80 N) to investigate the influence of normal load on the frictional response of non-dilative interface system. Steel and geomembrane continuum materials were used to investigate the influence of the hardness of the continuum material. The results of the experiments show that the frictional response of the interface systems varies with the normal load and the hardness of the continuum material. It is also observed that the shearing mechanism (sliding or plowing) at the interface is significantly influenced by the hardness of the continuum material and the normal load.

Keywords: Non-dilative interfaces, Frictional mechanism, Micromechanical behavior, Tribometer

1 Introduction

The importance of non-dilative interface system behavior is found in many geotechnical engineering applications such as smooth landfill liners, skin friction piles and friction based in-situ soil characterization devices[1–4]. The non-dilative interfaces are the weakest plane of failure for many geotechnical structures and the interaction at the interface is complex and can profoundly influence their energy efficiency, stability, and performance. The transfer of load from the geotechnical structures to the surrounding soils is mainly through friction, however, they do not obey Amontons' law of frictions [5]. The frictional mechanism is governed by the sliding and plowing mechanism without dilation at the interface and thus, traditional soil mechanics concepts are not sufficient to describe their underlying shearing mechanism. Previously, researchers have studied the influence of particle and continuum material properties and testing conditions on the macro response of non-dilative interface system [6–8]. Vangla and Gali [9]

revealed that interface shear response is governed by the particle contacts at the interface level. Therefore, understanding the shear behavior of a non-dilative interface system requires studying fundamental aspects that govern the macro aspects through the sliding and plowing of particulate materials on the surface of the continuum material at a micro-level that falls under tribology. The tribology literature is rich in studies on friction and wear [10–15]. However, only limited information applies to geotechnical composite systems. Thus, the principles of tribology can be extended to provide insight into particle surface interactions for developing better prediction models and an accurate understanding of the macro shear response of non-dilative interface systems.

This paper focuses on the investigation of the influence of normal load on the micromechanical shear behavior of a non-dilative interface system. To this end, a series of micromechanical interface shear experiments were conducted using a particle-on-disc tribometer. The experiments were conducted on glass bead and different continuum materials at different normal loads (5 N, 10 N, 20 N and 80 N) to investigate the frictional behavior. Steel and geomembrane were selected as the continuum material to address the effect of hardness of continuum material on the frictional behavior of non-dilative interface system. Further, the evolution of the friction coefficient due to surface wear was investigated in this study.

2 Experimental Methods and Procedure

2.1 Experimental Setup

A pin-on-disk multi-function tribometer model MFT5000 by Rtec instruments, available in the department of materials science and engineering of IIT Delhi was used to conduct the interface shear tests of single particle with different continuum materials. The apparatus with all the major components labelled is shown in Figure 1. The device allows a single particle to travel in the same circular path over the continuum material repeatedly while applying the constant normal load on the particle. The rotary drive of the tribometer is equipped with an automatic recognition feature, optimized torque, and proportional integral derivative values to maintain strict control on the testing parameters such as normal load and displacement rate. The device allows the adjustment of the of the rotary drive through movement in XY stage. The continuum material sample holder can be adjusted to accommodate the continuum material samples of different sizes. The particle is fixed to the instrumented arm using a collet to permit only the sliding of the particle and restrict rolling of the particle. However, the cantilever arm of the instrument is free to move in a vertical plane while shearing. The normal load is applied to the cantilever arm with a precision air cylinder and independently measured with a miniature load cell. The horizontal forces developed while shearing the particle is measured with strain gauges mounted on the arm in a full-bridge configuration. The inline optical profilometer is provided in the setup to measure the roughness of the surface during the test itself. Further, to maintain the constant environmental conditions throughout the test, the environment control unit is provided at the bottom of the system. The software provided by the Rtec instruments along with data acquisition system is used to record the data produced during the tests.

2.2 Materials and Characterization

For this study, glass bead (GB) is selected as the particulate material and two different types of continuum material, namely steel (ST) and geomembrane (GM) are selected to test two different types of interface contacts (GB-ST, GB-GM). A total of 10 particles of GB of average size of 2-3 mm were selected for particle-scale experiments. The particles' physical appearance, as shown in Figure 2 (a), demonstrates the spherical shape of GB. The image-based shape characterization proposed by Vangla, Roy, and Gali [16] was used in this study to characterize the shape of GB. To this end, digital images of the 10 particles at the same magnification were taken and analyzed. The average sphericity and roundness values for the GB are 0.96 and 0.99, respectively. According to the standard particle shape reference charts compiled by Santamarina and Cho [17], GB can be classified as rounded. Further, the GB particles were examined under a microscope and observed to be free of microfractures.

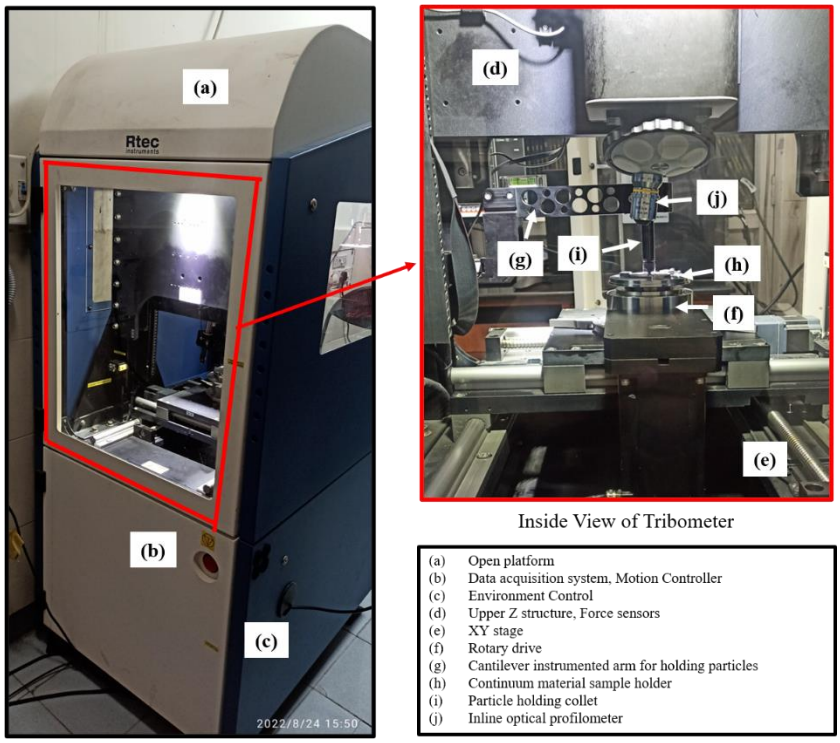

Figure 1. Multi-function tribometer used for conducting interface shear tests of single particle in this study

ST and GM were used as continuum material due to their applicability in geotechnical engineering and to obtain a range of hardness values. The physical appearance of the continuum materials used for this study is shown in Figure 2 (b). The ST surface was polished to eliminate the effect of roughness on the response. The average roughness measured using stylus profilometer of ST after polishing and GM was 0.567 µm and 0.347 µm, respectively. The average roughness of ST was comparable to GM after polishing. The hardness of the ST surface was determined using the Vickers hardness

test. The load of 4.903 N was applied for a dwell time of 12 s. The hardness of GM was determined using Shore-D hardness, applying the load of 0.005 N. A total of 10 indentations were made on each surface, and the average hardness value was calculated. The hardness of the ST and GM were 2.5 GPa and 0.057 GPa, respectively; thus, the hardness of ST was significantly high compared to the hardness of the GM.

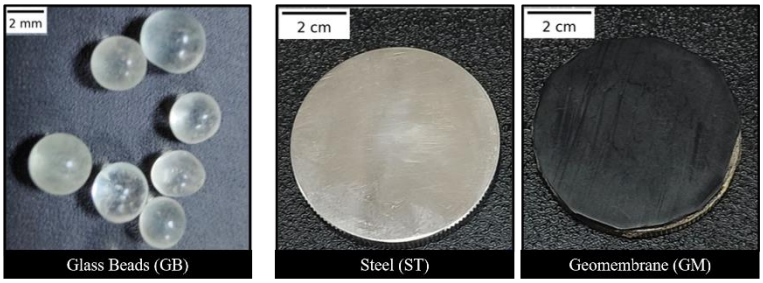

Figure 2. Materials used in this study (a) Particulate material (b) Continuum material

2.3 Sample Preparation and Testing Procedure

Sample preparation: The continuum material samples were made circular (50 mm diameter) with knurling at the edges to provide a firm grip for clamping them to the sample holder of the rotary drive. The ST surface was cleaned in an ultrasonicator bath at 50˚ C for 5 minutes to remove the impurities present on the surface. Then, ST sample was allowed to dry after wiping the surface with clean tissue paper. Due to the low hardness of GM, it was epoxy-glued to the mild steel circular backing plate (50 mm diameter) for clamping it to the sample holder of the rotary drive. The GM surface was cleaned with wet and dry clothes to remove the impurities present on the surface. The particulate materials GB were also cleaned in an ultrasonicator bath at 50˚ C for 5 minutes to remove the impurities and oven-dried before the tests. After the samples were cleaned, caution was taken for not touching the surface with bare hands while placing the samples. The continuum material samples were clamped rigidly using the clamps provided on the rotary drive sample holder. The glass bead was fixed on the instrumented cantilever arm using a collet to allow only sliding and was made in contact with the continuum material sample. The final testing configuration of particle-continuum material looks as shown in Figure 3.

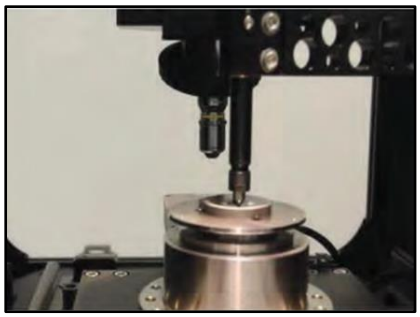

Figure 3. Final testing configuration of particle-continuum material

The normal load (5 N, 10 N, 20 N, 40 N, and 80N) was applied at the interface contact to the cantilever arm with a precision air cylinder. The continuum material sample was rotated at the fixed rate of 1 mm/minute for 6 revolutions, and the particle remained stationary during the test. The test was conducted for 6 revolutions to model in tribometer the field condition. The field condition is explained using a geomembrane sample after the interface test shown in Figure 4, and it is evident that the surface wear is different in three zones (a, b, and c). Zone a and c are low roughness zones whereas zone b is high roughness zone. The surface wear is maximum in zone b and thus a maximum number of particles pass through this zone leading to incremental surface wear. In zones a and b, a smaller number of particles pass compared to zone c, and thus surface wear is less. The same field condition is modelled in the tribometer experiments by conducting the tests for six revolutions. The horizontal forces developed while shearing was measured with strain gauges mounted on the arm in a full-bridge configuration and recorded by the Rtec instrumentations software. The inline optical profilometer in the device was used to quantify the roughness of the continuum materials before and after the test and to relate the degree of wear to the friction coefficient.

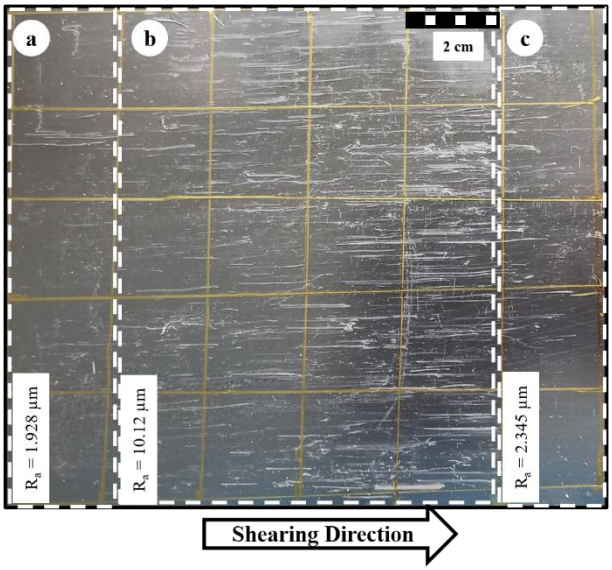

Figure 4. Geomembrane sample after interface shear test

3 Results and Discussion

A series of interface shear experiments were conducted using a particle-on-disc tribometer on different interface systems (GB-ST and GB-GM) at different normal loads (5 N, 10 N, 20 N and 80 N) to investigate the effect of normal load and continuum material hardness on the frictional response of non-dilative interface system. Further, the evolution of the friction coefficient due to surface wear was investigated in this study by conducting the test for six revolutions. Figure 5 presents the typical response of normal force-number of revolutions while shearing. It is observed from the response that the normal force remains constant throughout the shearing and thus, the apparatus

maintains a strict control on the testing parameters. A total of 10 particles were tested for each test condition and an average of the 10 friction coefficient values is plotted in Figure *7*.

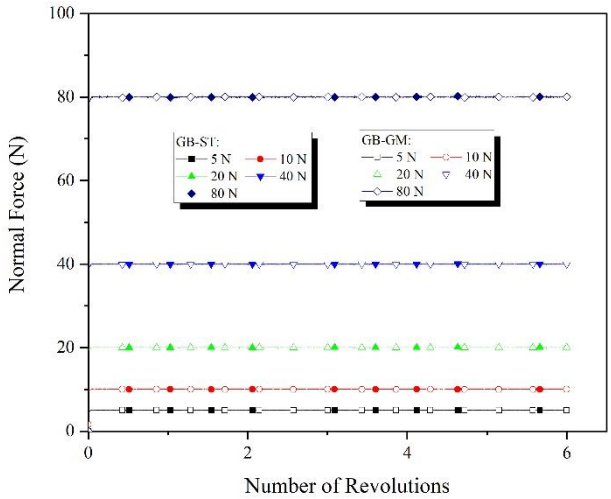

Figure 5. Normal force vs. number of revolutions response recorded while shearing of the particles for GB-ST and GB-GM interface system

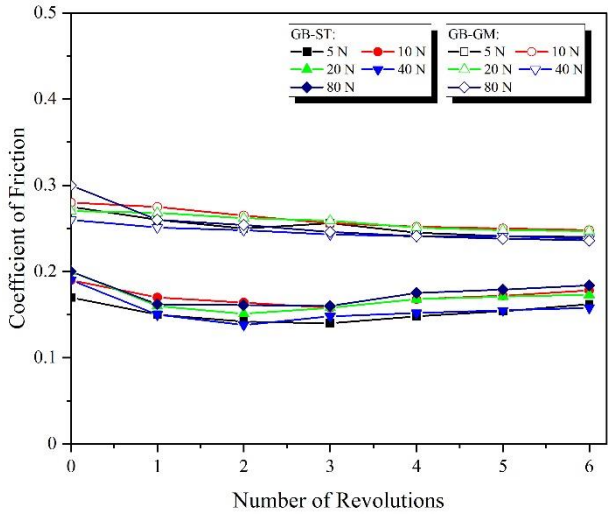

Figure 6. Coefficient of friction vs. number of revolutions response recorded while shearing of the particles for GB-ST and GB-GM interface system

Figure 6 presents the average coefficient of friction value vs. number of revolutions at different normal loads for GB particles tested with ST and GM. It is observed from the figure that the coefficient of friction value for GB-ST interface initially decreases and then increases after 2 revolutions at all the normal loads. However, in the case of the GB-GM interface, the coefficient of friction decreases from the peak value and then becomes almost constant at all the normal loads. The behavior of GB-ST response is

different compared to GB-GM as in the case of metals, the debris formed due to shearing gets entrapped in the asperities [18]. Thus, with an increase in the number of revolutions the friction coefficient increases due to the interaction of the wear debris from the ST surface with GB. However, in the case of GB-GM, with an increase in the number of revolutions, the friction coefficient decreases due to a decrease in the surface wear rate [19].

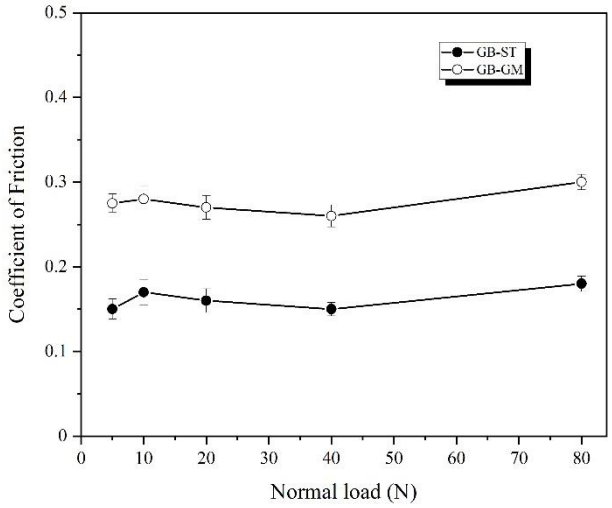

Figure 7. Coefficient of friction vs. normal load response for the interface contacts examined in this study

To demonstrate the effect of normal load on the shear response of geomaterial contacts, the average friction coefficient vs. normal load response is presented in Figure 7. It is observed that the friction coefficient initially increases with increase in normal load from 5 N to 10 N. Further it is observed that with the increase in normal load, the friction coefficient initially decreases and then increases for both the interface contacts. A similar trend has been reported by Dove and Frost [5] for the interface test of geomaterial contacts at the macroscopic level. The initial increase at 10 N may be attributed to the proper surface interaction between the asperities which may not be there at low normal load of 5 N [20, 21]. Further decrease in coefficient of friction for GB-ST and GB-GM is due to the non-linear increase in contact area with an increase in normal load and, thus, not obeying Amonton's law [10]. A further increase in the coefficient of friction is observed due to the change in mechanism from sliding to plowing [21, 22], where the contact stress exceeds the yield pressure of the material in contact. The critical normal load at which the mechanism changes from sliding to plowing depends on the type of interface contacts [5]. It is observed that incase of GB-GM, the increase in coefficient of friction after plowing is comparatively higher as compared to GB-ST which is due to low hardness of GM and comparatively more plowing due to deeper grooves formed. The mechanism changes from sliding to plowing is further manifested through roughness profiles obtained using profilometer. A typical surface profile of metal surface before and after shearing is shown in Figure 8. The average roughness value of both the surfaces before and after shearing is reported in Table 1. The average roughness values of shear-induced surface changes are increasing with an increase in normal load and

much change in value is observed at 80 N due to the contact stress exceeding the yield stress of the materials. Further, the average roughness is more in GM compared to ST surface due to lower hardness of materials resulting in deeper grooves formed because of surface damage.

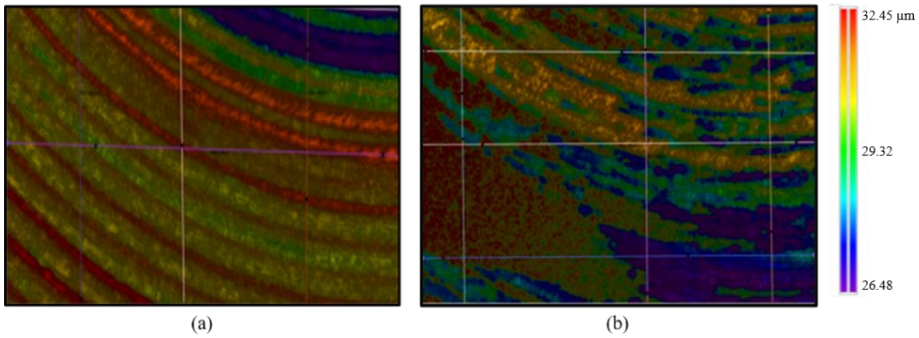

Figure 8. Surface roughness profile of ST surface obtained (a) before shearing and (b) after shearing at 80 N

Table 1. Average roughness values of the interface contacts before and after shearing at different normal loads

Interface Contacts	Average roughness before shearing (µm)	Average roughness after shearing (µm)				
		5 N	10 N	20 N	40 N	80 N
GB-ST	0.567	0.608	0.698	0.789	0.796	1.236
GB-GM	0.347	0.398	0.595	0.630	0.695	1.678

4 Conclusions

Micromechanical interface shear experiments were conducted to understand the fundamental shearing mechanism in non-dilative interface system. It is concluded that the frictional coefficient is dependent on the shearing mechanism which further depends on the normal load and hardness of the continuum material. Further, the study reveals that with increase in surface damage over the time the coefficient of friction decreases for GM and then reaches steady state, however, in case of ST, the friction coefficient initially decreases and then increases with the number of revolutions. Further, the difference in the polymeric material in contrast to metals highlights the importance of comparative study before using the concepts of tribology directly in geotechnical applications. This study provides experimental laboratory data to validate the numerical models and highlights the significance of incorporating the plowing models for economical designs of non-dilative interface system.

References

1. Lashkari A (2013) Prediction of the shaft resistance of nondisplacement piles in sand. Int J Numer Anal Methods Geomech 37:904–931. https://doi.org/10.1002/nag.1129
2. Pellet-Beaucour AL, Kastner R (2002) Experimental and analytical study of friction forces during microtunneling operations. Tunn Undergr Sp Technol 17:83–97. https://doi.org/10.1016/S0886-7798(01)00044-X
3. DeJong JT, Frost JD (2002) A multisleeve friction attachment for the cone penetrometer. Geotech Test J 25:111–127. https://doi.org/10.1520/gtj11355j
4. Stark TD, Poeppel AR (1994) Landfill liner interface strengths from torsional-ring-shear tests. J Geotech Eng 120:597–615
5. Dove JE, Frost JD (1999) Peak friction behavior of smooth geomembrane-particle interfaces. J Geotech Geoenvironmental Eng 125:544–555. https://doi.org/10.1061/(ASCE)1090-0241(1999)125:7(544)
6. Zettler TE, Frost JD, DeJong JT (2000) Shear-induced changes in smooth HDPE geomembrane surface topography. Geosynth Int 7:243–267. https://doi.org/10.1680/gein.7.0174
7. Fuggle AR (2011) Geomaterial gradation influences on interface shear behavior
8. Uesugi M, Kishida H (1986) Influential factors of friction between steel and dry sands. Soils Found 26:33–46. https://doi.org/10.3208/sandf1972.26.2_33
9. Vangla P, Gali ML (2016) Shear behavior of sand-smooth geomembrane interfaces through micro-topographical analysis. Geotext Geomembranes 44:592–603. https://doi.org/10.1016/j.geotexmem.2016.04.001
10. Bowden FP, Moore AJW, Tabor D (1943) The Ploughing and Adhesion of Sliding Metals. J Appl Phys 14:80–91. https://doi.org/10.1063/1.1714954
11. Sandeep CS, Senetakis K (2017) Exploring the micromechanical sliding behavior of typical quartz grains and completely decomposed volcanic granules subjected to repeating shearing. Energies 10:. https://doi.org/10.3390/en10030370
12. Li J, Zhou F, Wang X (2011) Modify the friction between steel ball and PDMS disk under water lubrication by surface texturing. Meccanica 46:499–507. https://doi.org/10.1007/s11012-010-9298-8
13. Kim HI, Lince JR, Eryilmaz OL, Erdemir A (2006) Environmental effects on the friction of hydrogenated DLC films. Tribol Lett 21:51–56. https://doi.org/10.1007/s11249-005-9008-1
14. Berman A, Drummond C, Israelachvili J (1998) Amontons' law at the molecular level. Tribol Lett 4:95–101. https://doi.org/10.1023/A:1019103205079
15. Marjanovic N, Tadic B, Ivkovic B, Mitrovic S (2006) Design of modern concept tribometer with circular and reciprocating movement. Tribol Ind 28:3–8
16. Vangla P, Roy N, Gali ML (2018) Image based shape characterization of granular materials and its effect on kinematics of particle motion. Granul Matter 20:. https://doi.org/10.1007/s10035-017-0776-8
17. Santamarina JC, Cho GC (2001) Determination of Critical State Parameters in Sandy Soils - Simple Procedure. Geotech Test J 24:185–192. https://doi.org/10.1520/gtj11338j
18. Menezes PL, Ingole SP, Nosonovsky M, et al (2013) Tribology for scientists and engineers: From basics to advanced concepts
19. Dove J, Bents D, Wang J, Gao B (2006) Particle-scale surface interactions of non-dilative interface systems. Geotext Geomembranes 24:156–168.

https://doi.org/10.1016/j.geotexmem.2006.01.002

20. Johnson KL (1982) One Hundred Years of Hertz Contact. Proc Inst Mech Eng 196:363–378. https://doi.org/10.1243/PIME_PROC_1982_196_039_02
21. Merz R, Brodyanski A, Kopnarski M (2015) On the role of oxidation in tribological contacts under environmental conditions. Conf Pap Sci 2015:1–11. https://doi.org/10.1155/2015/515498
22. Shooter KV, Tabor D (1952) The frictional properties of plastics. In: Proceedings of the Physical Society